ACS APPLIED MATERIALS & INTERFACES

www.acsami.org

Research Article

Adsorption and Diffusion Moderated by Polycationic Polymers during Electrodeposition of Zinc

Gastelle F. Tiétcha, Laura L. E. Mears,* Dominik Dworschak, Marcel Roth, Ingo Klüppel,* and Markus Valtiner*

Cite This: *ACS Appl. Mater. Interfaces* 2020, 12, 29928–29936

Read Online

ACCESS | Metrics & More | Article Recommendations

ABSTRACT: Electrodeposition of metals is relevant to much of materials research including catalysis, batteries, antifouling, and anticorrosion coatings. The sacrificial characteristics of zinc used as a protection for ferrous substrates is a central corrosion protection strategy used in automotive, aviation, and DIY industries. Zinc layers are often used for protection by application to a base metal in a hot dip galvanizing step; however, there is a significant interest in less energy and material intense electroplating strategies for zinc. At present, large-scale electroplating is mostly done from acidic zinc solutions, which contain potentially toxic and harmful additives. Alkaline electroplating of zinc offers a route to using environment-friendly green additives. Within the scope of this study an electrolyte containing soluble zinc hydroxide compound and a polyquarternium polymer as additive were studied during zinc deposition on gold model surfaces. Cyclic voltammetry experiments and in-situ electrochemical quartz crystal microbalance with dissipation (QCM-D) measurements were combined to provide a detailed understanding of fundamental steps that occur during polymer-mediated alkaline zinc electroplating. Data indicate that a zincate-loaded polymer can adsorb within the inner sphere of the electric double layer, which lowers the electrostatic penalty of the zincate approach to a negatively charged surface. X-ray photoelectron spectroscopy also supports the assertion that the zincate-loaded polymer is brought tightly to the surface. We also find an initial polymer depletion followed by an active deposition moderation via control of the zincate diffusion through the adsorbed polymer.

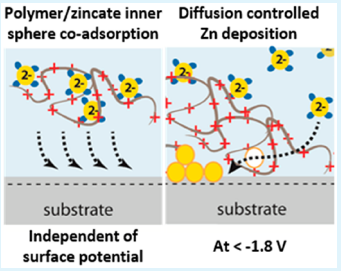

KEYWORDS: *electroplating, corrosion protection, polyamine, polymer additive, electrochemical QCM-D*

1. INTRODUCTION

Electroplating of zinc is an industrial process used to produce a protection layer on a ferrous substrate. Zinc deposition and dissolution[1−3] processes are widely studied. Owing to its more negative standard electrode potential (in contrast to iron), zinc will corrode preferably to the steel to produce a sacrificial protection of the substrate.[4−7] Zinc deposition is also utilized in the growing fields of novel rechargeable battery design[8,9] and CO_2 reduction.[10] For large-scale applications a central hurdle of the electroplating process is control of the local deposition rate. In several industries, complex substrate geometries result in high/low field regions with significantly varying local deposition rates. Controlling and steering the local process can provide real benefits to manufacturers, in particular via targeted control of deposition rates through an inhibition at high current densities and an acceleration at low current densities. This results in an even thickness distribution and a smooth and bright appearance of the zinc layer.

Because of its amphoteric property, zinc is soluble in both alkaline and acidic conditions as well as novel neutral[11] and nonaqueous electrolytes.[12] For electroplating this enables the deposition of zinc from both alkaline and acidic electrolytes. There are three main electrolytes used: alkaline cyanide, alkaline non-cyanide, and acidic electrolytes.[13,14] Today alkaline cyanide-based chemistry is rarely used because of its toxicity. Alkaline non-cyanide electrolytes were developed as nontoxic alternatives and are the focus of the present work.

A typical alkaline electrolyte is prepared by dissolving zinc oxide in sodium or potassium hydroxide solution to form $[Zn(OH)_4]^{2-}$ (zincate) complexes. Jelinek et al. show that the complex $[Zn(OH)_4]^{2-}$ is formed in these electrolytes.[13] Spectroscopy measurements also provide evidence that only $[Zn(OH)_4]^{2-}$ is formed when preparing alkaline zinc electrolytes.[15,16] Also measuring the redox potential of zinc in strongly alkaline electrolytes further supports the formation of $[Zn(OH)_4]^{2-}$.[17] It is important to note that the formation of the tetrahydroxo zincate complex only appears in highly concentrated alkali hydroxide solution (an excess of hydroxide ions is needed). In contrast to this, the formation of $[Zn(OH)]^+$, $[Zn(OH)_2]$, or $[Zn(OH)_3]^-$ is favored in less alkaline conditions.[18]

Received: March 5, 2020
Accepted: May 29, 2020
Published: May 29, 2020

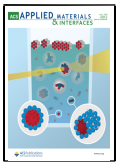

https://dx.doi.org/10.1021/acsami.0c04263
ACS Appl. Mater. Interfaces 2020, 12, 29928−29936

The mechanism of Zn deposition is debated controversially. Some authors claim that the zinc reduction happens as a one-step electron-transfer reaction:[19,20]

$$Zn(OH)_2 + 2e^- \rightarrow Zn + 2OH^- \quad (1)$$

while others propose a two-electron process as follows:[13]

$$Zn(OH)_2 + e^- \rightarrow ZnOH + OH^- \quad (2)$$

$$ZnOH + e^- \rightarrow Zn + OH^- \quad (3)$$

Indeed, other studies show that the reaction of the zinc electroreduction is more complex and may proceed through a four-step mechanism starting from the tetrahydroxo complex as follows.[21−23]

$$[Zn(OH)_4]^{2-} \rightarrow [Zn(OH)_3]^- + OH^- \quad (4)$$

$$[Zn(OH)_3]^- + e^- \rightarrow [Zn(OH)_2]^- + OH^- \quad (5)$$

$$[Zn(OH)_2]^- \rightarrow ZnOH + OH^- \quad (6)$$

$$ZnOH + e^- \rightarrow Zn + OH^- \quad (7)$$

Although alkaline baths nowadays are environmentally benign, they have disadvantages, specifically the formation of powdery, dark, or spongy zinc layers. To overcome these problems and to improve the plating performance, additives can be utilized for moderating the crystal growth.[24−26] A number of additives show excellent performance. For instance, Ortiz-Apericio et al.[27] show a beneficial influence of vanilin and anisaldehyde on the electrochemical deposition and the layer morphology of a Zn−Co alloy. Poly(vinyl alcohol) addition also results in a grain refinement during the deposition.[28] Similarly, quaternary ammonium compounds (for example, tetraethylammonium hydroxide, tetrabutylammonium hydroxide, nicotinic acid, and *N*-benzyltriethylammonium) can effectively inhibit dendrite formation of zinc.[29]

Already, in 1972 Diggle and Damjanovic[30] realized the effect of quaternary alkylammonium salts on the dendrite formation during electrocrystallization of zinc and argued that two mechanisms are active. On the one hand, a physical blocking (steric) of the surface by the adsorbed inhibitor moderates deposition at highly catalytic sites.[31] On the other hand, the specific adsorption of the quarternary compounds modifies the diffuse layer, so that deposition kinetics, i.e. the position of the reaction planes is modified. The effect of specific adsorption of moderators was further confirmed by Oniciu and Mureşan.[24]

While it seems clear that adsorption of molecules can effectively moderate metal deposition, little is known about the molecular mechanism and moderation mechanism of other moderators, such as polymers, during electroplating.

The aim of this work is to fundamentally understand the effect of organic compounds, especially polyquaternary ammonium polymers, on the electrodeposition of zinc. This work investigates the behavior of polyquaternium 2 (PQ) as an additive for the alkaline zinc electrolyte, with the aim to unravel the mechanism by which it controls zinc deposition. Here cyclic voltammetry and quartz crystal microbalance with dissipation (QCM-D) measurements were performed to understand the adsorption mechanism and kinetics during the metal deposition and the role of the polymer in the alkaline electrolyte. Knowing this information can help to improve electrolyte systems in terms of both the material properties of the electroplated layer produced and their environmental impact.

2. EXPERIMENTAL SECTION

2.1. Chemicals and Materials. The zinc oxide (99.7% purity) and the NaOH solution (50%) were purchased from VWR, and the polyquarternium 2 (62 wt % in water) was from Sigma-Aldrich. All chemicals were used as received without further purification.

The alkaline non-cyanide zinc electrolyte was prepared by dissolving the zinc oxide in NaOH solution and using deionized water to achieve the desired concentration. The concentration in the bath is 3.8 M for the NaOH and 0.2 M for the zinc. The polyquarternium 2 in the electrolyte is adjusted to 0.1 wt %.

2.2. Cyclic Voltammetry (CV). The zinc layer was deposited during cyclic voltammetry in a bulk electrochemistry on a gold model surface by using a GAMRY potentiostat/galvanostat/ZRA (interfaces 1010 E). During the experiments the solutions were bubbled continuously with argon. The working electrode was a molecularly smooth gold surface prepared by template stripping from 100 nm gold deposited on mica[32] with a geometrical area of 1 cm^2 and an RMS roughness well below 1 nm over several cm^2. The flat, glass supported electrode was contacted with a gold wire. Experiments were performed in a three-electrode setup in a cylindrical PEEK cell with platinum mesh as counter electrode and Ag/AgCl electrode (in 3 M KCl, in a Luggin capillary) as the reference. For each experiment fresh gold electrodes were stripped shortly before the experiment, and the working electrode was electrochemically further preconditioned in a 0.1 M NaOH solution by potential cycling (between −0.3 and 0.3 V vs Ag/AgCl). All measurements were made at a rate of 10 mV/s. The stability of the experiment was determined by measuring the OCP of the Ag/AgCl electrode over a time period of 6 h.

2.3. CV in a QCM-D Cell. The zinc deposition happened in an electrochemical QCM-D cell on a gold surface by using a GAMRY potentiostat/galvanostat/ZRA (interfaces 1010 E). The electrolytes were prepared as above and stored in plastic containers. During the experiment a Teflon beaker was used, and the solution was bubbled constantly with argon during experiments. The equipment (a Qsense E1) and the gold-coated quartz sensors (with an RMS roughness below 1 nm) were purchased from Biolin Scientific and used in the Qsense electrochemistry module. The experiments were performed at 24 °C under flow conditions, and the fifth overtone was used for the data analysis with the Sauerbrey equation to calculate the mass deposited. For the zinc and zinc with polyquarternium 2 electrolytes the Sauerbrey equation is appropriate;[33] for the polyquarternium 2 and background electrolytes the criterion is met to differing extents, and therefore the mass should be treated as indicative rather than quantitative. For the cyclic voltammetry part a platinum sheet and an Ag/AgCl electrode (in 3 M KCl) were used respectively as counter and reference electrodes. Every gold sensor was electrochemically polished in a 0.1 M NaOH solution before starting the experiment and used for one zinc deposition experiment only. Ten cycles were measured, and the last three cycles are plotted in this work. Transient chronoamperometric measurements were also made by using the same preparation protocol and returned to a dissolution potential between potential steps.

2.4. X-ray Photoelectron Spectroscopy. Gold substrates were prepared as for the bulk electrochemistry, and samples were prepared in polyquarternium 2 solution (removed at peak PQ2, approached by linear sweep voltammetry at 10 mV/s scan rate), in zinc with polyquarternium 2 both under the same conditions as the PQ sample and removed at −1.62 V at the beginning of the zinc deposition peak, and in the zinc electrolyte after a CV (0.05 to −1.5 V, 10 mV/s) removed at 0 V. Chemical composition and chemical states of the surface were determined by using the Axis Supra (Kratos Analytical) spectrometer.

No charge neutralization was used. XPS spectra were shifted with respect to gold at 83.95 eV. Spectra were taken with a resolution of 0.1 eV and a pass energy of 160 eV. All spectra were fitted by using reference compounds from the NIST database.[34,35]

https://dx.doi.org/10.1021/acsami.0c04263
ACS Appl. Mater. Interfaces 2020, 12, 29928−29936

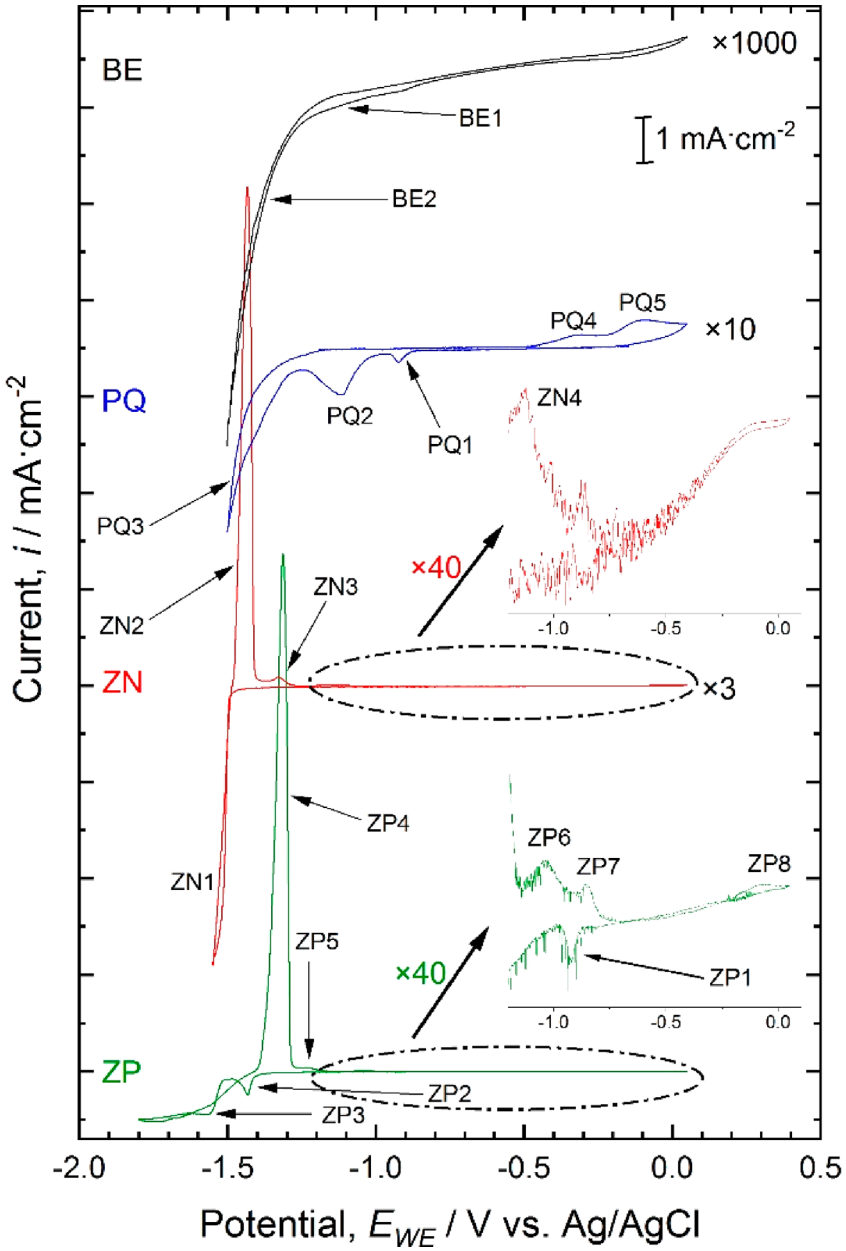

Figure 1. Full cyclic voltammogram (CV) of the electrolytes analyzed during this work. BE is a 1000 times magnification of the CV of NaOH. PQ is a 10 times magnification of the CV of the polyquarternium 2 dissolved in NaOH (0.1% solution). ZN is a 3 times magnification of the CV of the zinc electrolyte containing no polyquarternium 2. ZP is the CV of the zinc electrolyte with polyquarternium 2.

3. RESULTS AND DISCUSSION

In this work we studied the influence of polymer additives on zinc deposition from the alkaline zinc bath using both electrochemistry (cyclic voltammetry) and QCM-D measurements. The key questions that we try to answer are: how does the polymer influence the deposition mechanism, and how does this enable deposition of a thin, smooth, and bright zinc layer with optimized thickness?

Four electrolytes have been analyzed as shown in Figure 1: The background electrolyte NaOH (labeled BE), a solution of 0.1% polyquarternium 2 in NaOH (PQ), zinc electrolyte without polyquarternium 2 (ZN), and zinc electrolyte with 0.1% polyquarternium 2 (ZP). The characteristic cyclic voltammograms in the cathodic region on a gold electrode are compared. These data reveal a number of interesting aspects as follows.

Figure 1 BE shows the electrochemical behavior of a gold electrode in the NaOH electrolyte with two characteristic reduction peaks labeled BE1 and BE2. The first cathodic peak BE1 at −1.14 V vs Ag/AgCl is attributed to the adsorption of cations (H^+ and Na^+) at the electrode interface. At a potential of about −1.3 V the hydrogen evolution reaction (HER) starts to dominate.

In contrast for PQ, also shown in Figure 1, the CV indicates five peaks (PQ1, PQ2, and PQ3 in the cathodic sweep and PQ4 and PQ5 in the anodic sweep). The peaks PQ1 at −0.92 V and PQ2 at −1.12 V vs Ag/AgCl can be attributed to the electrosorption of the polymer. The intensity of PQ1 is smaller and may characterize low-molecular-weight compounds in the solution and residual oligomers formed during the synthesis. Alternatively, the combination of both peaks may be interpreted as an initial electrosorption with low coverage,

https://dx.doi.org/10.1021/acsami.0c04263
ACS Appl. Mater. Interfaces 2020, 12, 29928−29936

where the polymer remains in a mushroom regime, while the second peak may indicate a collapse of the adsorbed molecules into a more dense packing.

The adsorption or grafting of polymer chains on to a planar solid−liquid interface is a well-studied phenomenon.[36,37] Briefly, there are two main configurations or regimes depending on the density. At low surface density the mushroom regime describes the grafting of polymer chains to the interface without overlap between neighboring chains. This is possible when the surface density of anchored polymer Γ is smaller than $1/R_F^2$, where R_F is the Flory radius. Each chain is isolated from its neighbors with the average distance between grafting points larger than the radius of gyration. When the chains are adsorbed at high densities, the probability of obtaining a brush structure for the resulting layer is very high, especially when the neighboring chains are so close that they can overlap with each other.

Interestingly, also the HER is significantly altered and indicates an additional shoulder at about −1.35 V (PQ3). We interpret this as a moderation of the HER by the adsorbed polymer. Moderation is likely linked to a lower number of adsorption positions of water due to competitive polymer adsorption and a related change of the reaction mechanism and/or kinetics of the HER. This is an interesting insight and demonstrates that the positively charged polymer can effectively compete with or rather modify the kinetics of the HER. In the anodic sweep, the peaks PQ4 and PQ5 can be attributed to desorption of polyquarternium 2. This is obviously a highly nonideal electro(de)sorption process with a considerable overpotential, considering the potentials of the electrosorption peaks (PQ1 and PQ2). This is not unexpected for large molecules such as polymers.[38,39]

Comparing the pure zincate solution, ZN, in Figure 1 with the two other reference solutions shows one significant cathodic peak ZN1 and three anodic peaks ZN2, ZN3, and ZN4 at −1.43, −1.33, and −1.13 V vs Ag/AgCl, respectively. ZN1 is indicative of a competitive zinc deposition and HER. Interestingly, also the HER is shifted in the ZN solution and starts at −1.48 V vs Ag/AgCl, which is significantly more negative in comparison to BE and PQ. This indicates that the zincate in solution may result in an interfacial adsorption layer, i.e., an electric double-layer structure in this case, that modulates the hydrogen adsorption and consequently the HER kinetic pathways by competitive adsorption. The anodic peak ZN2 indicates the corresponding Zn dissolution peak during the anodic sweep.

Including both the polyquarternium 2 and the zincate in the ZP electrolyte results in significant changes to the cyclic voltammogram in Figure 1. Here, we find three cathodic peaks with those related to the zinc deposition, ZP2 and ZP3, appearing at significantly more cathodic potentials of −1.43 and −1.56 V vs Ag/AgCl, respectively, and five anodic peaks with the main zinc dissolution peak, ZP4, at −1.30 V vs Ag/AgCl. Compared to the zincate solution ZN, the Zn deposition is obviously actively moderated.

For interpreting this result, we will need to consider, first, how the polymer structure changes in the two different alkaline solutions and how it enables an effective Zn deposition. In alkaline solutions the polyquarternium polymer will be positively charged, as the quaternary amine is charged at all pH levels. This charge on the polymer will be screened by co-ion absorption (e.g., OH^-) into the polymer. In turn, the polymer will remain in a random coil structure, with a typical radius that depends on the contour length of the individual coils and the solubility. As the solubility is quite good, the radius can be estimated by using the Flory radius $R_F \sim I_s n^{0.6}$, where n is the number of segments and I_s the length of a segment.[40] As explained above, the R_F is the typical distance to which polymers can adsorb at surfaces without significant compacting and brush formation. If zincate is present, the zincate can easily coabsorb into the polymer, in an effective competition with hydroxide ions, to screen the charge of the polymer. There are two motifs that can result in significant uptake of zincate into an amine-based polymer. First, positively charged amine groups can interact with the negatively charged zincate, and second, amines can complex with the zincate directly. Given the quaternary amine structure of PQ, the first possibility seems more likely, while complexation is impossible with quaternary amines.[41,42] This coabsorption of zincate into the polymer enables its approach to a negatively charged surface, directly into the inner sphere of the electric double layer. Essentially the electrostatic penalty is lifted, enabling a controlled approach to the negatively charged surface at deposition potentials.

Now, considering such a Zn-loaded polymer structure, the CV peaks may be described as follows: the weaker positive charge of the polymer structure leads to corresponding electrosorption peak, ZP1, at −0.92 V to have a much lower current than in the PQ solution. ZP1 also appears to form a couple with ZP7 at −0.86 V. Consistent with this interpretation is the broad peak, ZP8, at ∼−0.06 V, which would correspond to PQ5, attributed to electrodesorption of the polymer in the PQ solution. The peak at ZP2 may hence indicate the deposition of the zinc that is absorbed within the positively charged polymer coil. The overall only weakly positively charged polymer aggregate enables an effective approach of zincate to the surface, without a significant electrostatic penalty. The peak structure clearly indicates a process that quickly depletes, which is in line with Zn depletion of the surface bound polymers. This first Zn deposition peak deposits an initial Zn layer at a 100 mV more anodic potential compared to Zn deposition in ZN solution. This is further indicative of a significant overpotential reduction for the Zn deposition, which supports a polymer-mediated activation of the zincate complex by coabsorption into the amine polymer coil. In addition, the second rise and plateau of the cathodic deposition current, at ZP3, is consistent with a Zn deposition that is moderated and rate limited by diffusion of zincate through the adsorbed and surface bound polymer. In particular, considering that this current levels and only weakly depends on the potential below about −1.6 V, a diffusion-controlled process moderation through the polymer is active in the combined system. The polymer is an effective surface coating that diffusion limits the zinc deposition by structural features of the polymer and its effective integration into the electric double layer at negative potentials.

Also the Zn dissolution peaks ZP4, ZP5, and ZP6 are shifted to more anodic potentials compared to dissolution from the ZN electrolyte, ZN2, ZN3, and ZN4.

XPS spectra in Figure 2 further support the mechanism of an initial loaded polymer bringing the zincate to the surface. Upon comparison of the ZP sample removed at the polymer deposition potential (polarized to a potential equivalent to peak PQ2) with the other ZP and ZN samples, there is a peak at a binding energy far lower than any reported in the NIST database for either metallic or zinc oxide or hydroxide.

https://dx.doi.org/10.1021/acsami.0c04263
ACS Appl. Mater. Interfaces 2020, 12, 29928−29936

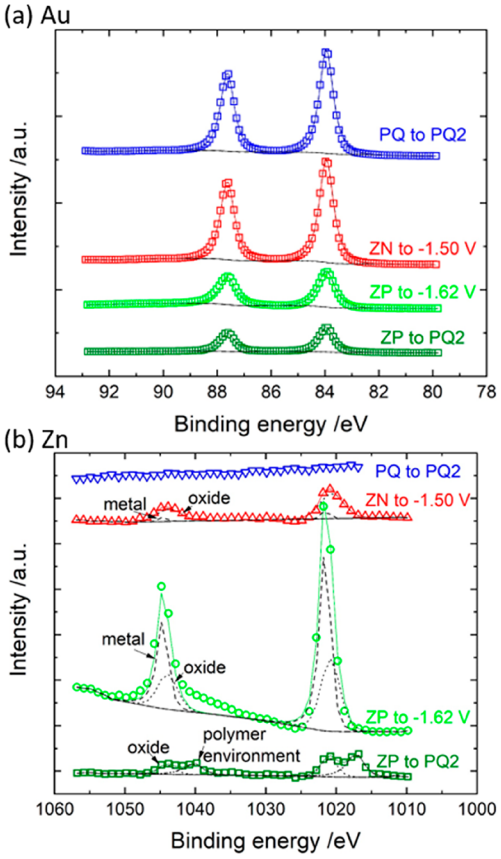

Figure 2. XPS spectra for (a) Au $4f_{7/2}$ and $4f_{5/2}$ and (b) Zn $2p_{3/2}$ and $2p_{1/2}$ electrons for gold electrodes in three different electrolytes: PQ polarized to the potential of peak PQ2, ZN polarized to −1.5 V (the start of deposition) but then removed at 0 V, and ZP polarized to and removed at both −1.62 V (the start of deposition) and the equivalent potential of peak PQ2. In (a) only metallic gold peak characteristics were required to fit the data. In (b) both metal and oxide characteristics are found for the ZN and ZP samples taken to deposition potentials, whereas the ZP sample polarized to the PQ adsorption potential exhibits an oxide peak and another assigned to the Zn species in the polymer environment.

Therefore, in Figure 2 and Table 1 we assign the peaks at 1017 and 1040 eV to zinc located within the polymer environment.

Table 1. Peak Positions for Fits to the Zn $2p_{3/2}$ and $2p_{1/2}$ XPS Spectra

position (eV) Zn $2p_{3/2}$|$2p_{1/2}$	metal	oxide	polymer environment
PQ to PQ2			
ZN to −1.5 V	1021.29|1044.31	1020.64|1043.75	
ZP to PQ2		1021.03|1044.03	1017.14|1040.14
ZP to −1.62 V	1021.48|1044.54	1020.83|1043.94	

There is a coexistence with the oxide which could have formed between preparation and measurement. There was also little evidence to suggest alloying of the zinc with the gold substrate[43] following polarization to deposition potentials in either ZN or ZP electrolytes.

While CVs and XPS already provide a detailed insight into the electrochemical mechanism at play, QCM-D experiments can further support arguments discussed above. In the following paragraphs, we discuss electrochemical QCM-D measurements with similar solutions and surfaces. This provides a direct view on the mass deposition during the zinc electroplating process. Figure 3 shows the variation of the current and the deposited mass and dissipation during cyclic voltammetry for all electrolytes examined for a potential window from −0.4 to −1.2 V vs Ag/AgCl, where no zinc is yet deposited. This is thereafter termed nonreactive cycling in the polymer adsorption/desorption region. Figure 4 goes further into the cycling of dissipation observed in ZP electrolyte. Later Figure 5 shows QCM-D data for active zinc deposition (with bulk deposition) from the zinc electrolyte without (ZN) and with polyquarternium 2 (ZP). The presented data indicate a number of interesting results as follows.

First, during nonreactive cycling with the background electrolyte, NaOH (Figure 3a-BE), the mass adsorbed to the gold surface increases and decreases, mirroring the trend of the current measured during cyclic voltammetry. The turning points coincide with those of the applied potential at −1.20 and −0.40 V vs Ag/AgCl. The changes are overlaid on top of a significant initial adsorption that is seen when cycling first begins. Here, the corresponding sharp decrease back to the baseline mass at OCP is seen in the figure after the final cycle finishes and the potential returns to OCP. The ions available in solution are Na^+ and OH^-; therefore, the mass increase must be attributed to charge regulation of these ions within the electric double layer (EDL). Upon cathodic polarization, the increasingly negative surface charge, σ, of the gold is compensated by an increasing adsorbed mass of sodium ions, as seen in the plot. Owing to the dissipative changes in the BE data, a full kinetic network model would be required to interpret the full viscoelastic behavior of the EDL.

Second, the PQ mass vs potential characteristic is shown in Figure 3a-PQ. The trend is similar compared to the BE with turning points at the applied potential −1.20 and −0.40 V vs Ag/AgCl. There are two notable differences compared to BE. First, the data also show a significant plateau region at anodic potentials, and no significant jump is observed upon switching back to OCP. This indicates that the positively charged polymer is likely physisorbed at all potentials, limiting the need for compensating any surface charge with sodium from the EDL. Second, the increase and the decrease of the adsorbed mass have a slightly steeper slope of mass vs potential. The slope change may indicate denser packing of polymers, with the higher physisorbed polymer mass reflected in the increased slope.

Third, Figure 3a-ZN describes the behavior of the zinc electrolyte without polyquarternium 2. As can be seen, compared to the first two solutions, the characteristic is completely different. There are flat plateau regions at more anodic potentials. The significant difference in mass between the more anodic and cathodic potentials indicates that the zincate electrolyte forms a significantly different electric double layer compared to the simple EDL charging observed in pure NaOH (BE). At a critical potential of about −1 V ions may compact at the inner Helmholtz plane of the electric double layer, increasing the effective mass on the electrode, while no additional stepwise current flows.

Finally, Figure 3a-ZP corresponds to the current and mass plots for the zinc electrolyte with polyquarternium 2 (ZP). Here we find a completely different characteristic. Three peaks are visible for every cycle. The mass plot (thin line) appears to be a qualitative addition of effects seen for both the zinc electrolyte without polymer (ZN) and the polymer solution

https://dx.doi.org/10.1021/acsami.0c04263
ACS Appl. Mater. Interfaces 2020, 12, 29928−29936

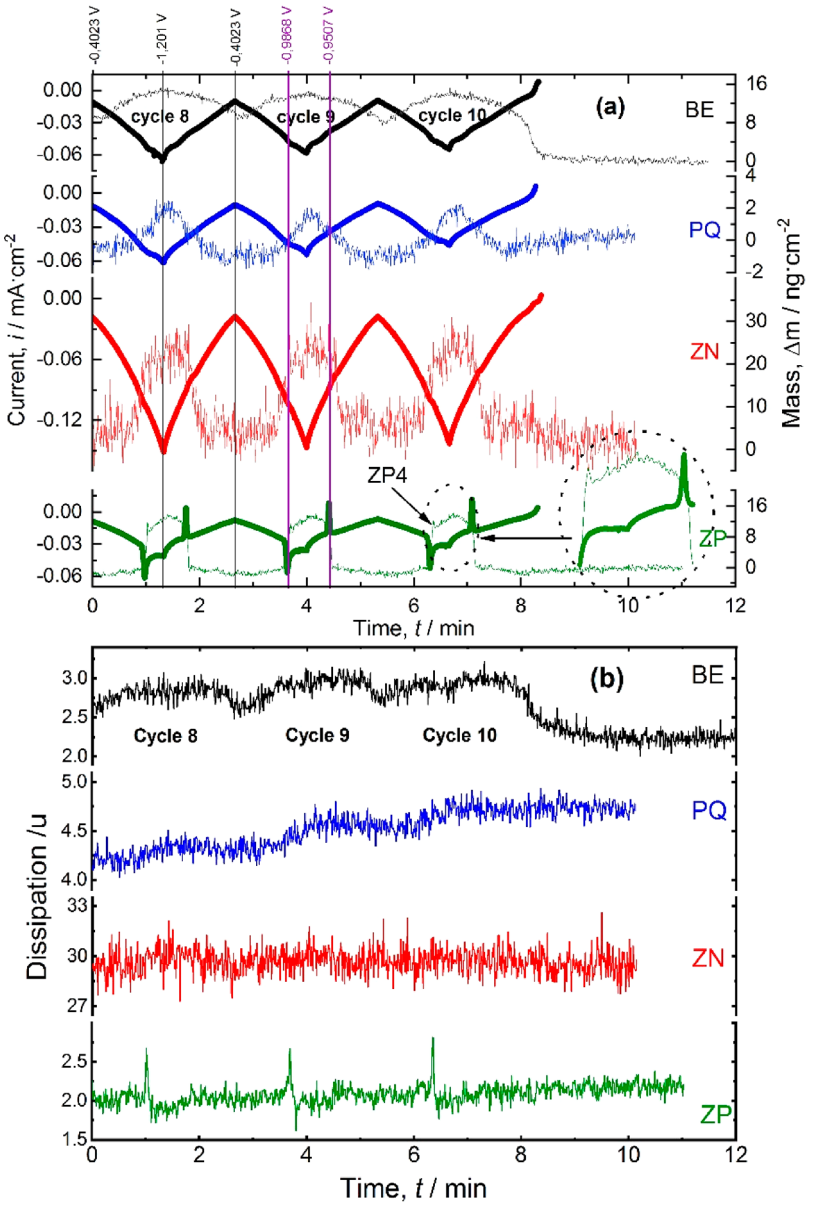

Figure 3. Nonreactive cycling (cycling between −0.4 and −1.2 V vs Ag/AgCl). (a) Current and mass against the time for all electrolytes. Thick lines correspond to the current plots; thin lines correspond to the mass plots. (b) Dissipation behavior vs time for all electrolytes. BE: NaOH electrolyte; PQ: 0.1% solution of polyquarternium 2 in NaOH; ZN: zinc electrolyte without polyquarternium 2; ZP: zinc electrolyte with polyquarternium 2. Note for the BE the mass should be treated as indicative rather than quantitative (see the Experimental Section).

(PQ). Similar to ZN, we see an initial plateau followed by a steep mass increase at a critical potential of about −1 V (labeled with ZP4). After steep increase, the mass first decreases slightly and then follows the trend of the adsorbed polymer.

We interpret the steep increase at −1 V as the proposed initial electrosorption of a zincate-loaded polymer. In contrast to the pure polymer, we find a subsequent short drop in mass indicating an initial electrosorption and a subsequent depletion of the polymer. Afterward, a mass increase similar to that of the polymer solution, and no plateau region, are observed. This agrees with a compacting of the now depleted polymer. Also, this is in line with the simultaneously measured dissipation. Figure 3b shows the dissipation as a function of the time (i.e., applied potential) during repetitive CV cycling within the electrochemical window from −0.4 to −1.2 V. The background electrolyte, the PQ solution, and the neat zincate solution show no particular significant features in the dissipation. All solutions, except the pure zincate solution (ZN), indicate a transient increase of the dissipation within the first few cycles, indicating a surface annealing.[44] Only data for the ZP electrolyte indicate a swift increase, followed by a decrease of the dissipation back to the baseline, upon the initial adsorption of the Zn-loaded polymer. The process occurs over a few points in the QCM-D data, which is recorded every 0.4 s. Each point is therefore 10 times longer in time than the Zimm time, which is calculated as 0.36 ms. The Zimm relaxation time[45] is how long the polymer requires to explore its full configuration space once. Hence, the sharp increase in dissipation occurs over a longer time than the natural fluctuations of the polymer configuration. Figure 4 provides another way to visualize this process via a mass vs dissipation plot and the changes

https://dx.doi.org/10.1021/acsami.0c04263
ACS Appl. Mater. Interfaces 2020, 12, 29928−29936

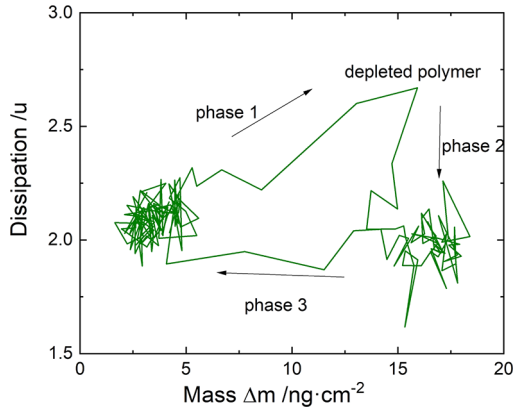

Figure 4. Mass vs dissipation plot for one cycle of the QCM-D measurement of the ZP electrolyte shown in Figure 2. The arrows indicate the direction of the cycle with time. The three phases are described in the text.

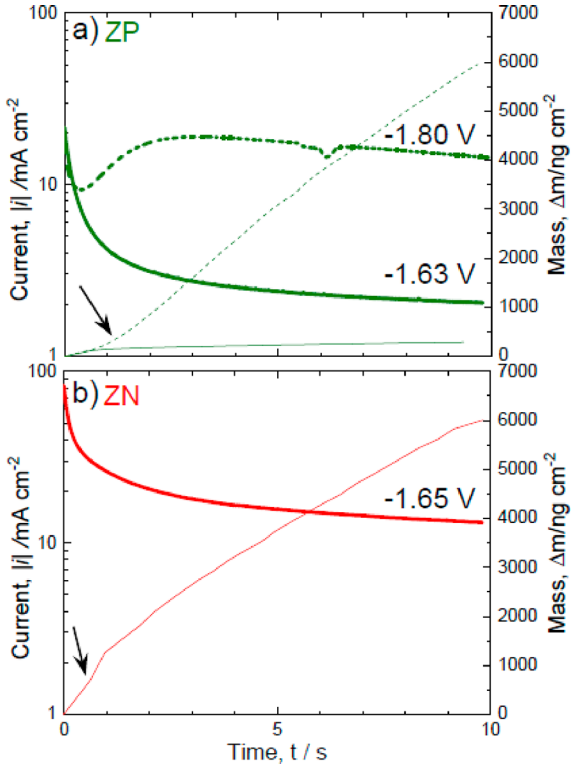

Figure 5. Current and mass transient data during potentiostatic Zn deposition from (a) ZP (solid lines at −1.63 V and dashed lines at −1.80 V) and (b) ZN, respectively. Thick lines correspond to the current, and thin lines represent the change in mass.

happening to the polymer chains at the interface triggered by the potential change. The dissipation and mass increase at the same time (phase 1 in Figure 4) as the loaded polymer adsorbs and rapidly undergoes an initial depletion of its load onto the surface.

The depletion is a transient state and dissipation decreases (phase 2) as the polymer stiffens as it reloads with zincate and the surface configuration equilibrates. When the charge is more positive, the zincate (and polymer) is released from the surface, and the mass decreases once more (phase 3). Again this is a strong indication for an initial adsorption, followed by a Zn depletion (due to zincate or zinc adsorption to the metal surface). This effectively modulates the stiffness of the adsorbed polymer, consistent with the observed dissipation fluctuation.

As such we can confirm that the polymer and also the zincate-loaded polymer adsorb at the electrode surface. Effectively, the polymer will hence moderate the deposition at lower potentials from −1.4 to −1.8 V, which is further shown in Figure 5. Specifically, Figure 5a shows representative results of potentiostatic Zn deposition from ZP and Figure 5b from ZN recorded in a QCM-D. At −1.6 V deposition from the ZP solution shows rather limited mass gain and a fast drop of the current. Compared to the data for ZN, without the polymer (see Figure 5b), the data for ZP at −1.6 V suggest a considerable slowdown of the deposition rate, which is consistent with almost all of the mass deposited deriving from the initial polymer depletion at the interface. Interestingly, and as shown in Figure 5a, deposition from ZP initiated at −1.8 V indicates a fast initial drop of the deposition rate, followed by a subsequent rise of the rate. This change of the deposition rate also coincides with a significant change of the mass deposition rate (marked by an arrow). The mass gain is initially slow and also much slower in comparison to the rate in the ZN solution (compare rates which are marked by the arrows), which is consistent with an initial and fast depletion of the zincate from the polymer in the ZP solution. The subsequent rise of the current and mass deposition rate clearly suggests a diffusion-controlled deposition following the initial depletion.

4. CONCLUSION

A Zn-plating electrolyte contains negatively charged zincate complexes $[Zn(OH)_4]^{2-}$ that, in principle, cannot easily approach a negatively charged electrode surface due to electrostatic repulsion. Figure 6a shows a schematic of the electric double layer in ZN solution, which mainly consists of sodium co-ions at cathodic potentials where the surface carries a large negative charge, σ. As a result, zincate can only deposit through an outer-sphere reaction. This offers very little to no direct steering and control of the reaction rates.

As indicated in Figure 6b, the PQ polymer coils, on the other hand, are generally positively charged (due to the quaternary amine) and can hence easily approach and adsorb at the gold surface, effectively competing with sodium co-ions in the inner sphere of the electric double layer.

Also, PQ can absorb zincate ions forming a zincate loaded and likely still weakly positively charged polymer. This allows the negatively charged zincate to coadsorb to the surface in the inner sphere of the electric double layer. Potential central steps of the mechanism for Zn plating moderated by PQ are also depicted in Figure 6b and can be summarized as follows. In step 1 the zincate/PQ aggregate can easily transport zincate to the surface with a low electrostatic penalty. Close to the surface, essentially in the inner sphere of the electric double layer, the reduction mechanism described in step 2 can then reduce the zincate ions, while depleting zincate within the adsorbed polymer layer. Yet the polymer film remains at the interface. In step 3 this layer then effectively acts as a moderator of the reduction reaction due to a targeted control of the zincate diffusion through the polymer. Our findings offer interesting insight into how one may tune and control the polymer for making more effective additives for Zn plating and electrodeposition in general.

https://dx.doi.org/10.1021/acsami.0c04263
ACS Appl. Mater. Interfaces 2020, 12, 29928−29936

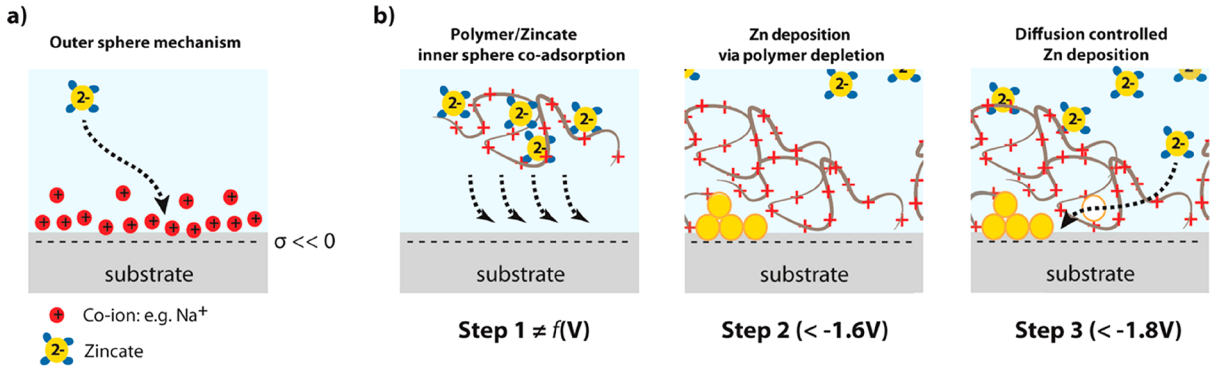

Figure 6. Schematic understanding of the PQ-controlled zinc deposition. (a) From ZN solutions the Zn deposition proceeds via an outer-sphere reaction. Because of the high negative surface charge, σ, the inner electric double layer consists mainly of sodium co-ions. (b) In ZP solutions a three-step mechanism proceeds via (1) coadsorption of zincate together with the positively charged polymer, which effectively competes with sodium co-ions in the inner sphere of the electric double layer, (2) during electrodeposition zinc initially deposits via depletion of zincate from the adsorbed polymer, and (3) the depleted polymer subsequently establishes a diffusion barrier, which moderates the ongoing deposition, improving the layer quality.

AUTHOR INFORMATION

Corresponding Authors

Laura L. E. Mears − *Institute of Applied Physics, Vienna University of Technology, Vienna A-1040, Austria;* orcid.org/0000-0001-7558-9399; Email: laura.mears@tuwien.ac.at

Ingo Klüppel − *Dörken MKS-Systeme GmbH & Co. KG, D-58313 Herdecke, Germany*; Email: iklueppel@doerken.de

Markus Valtiner − *Institute of Applied Physics, Vienna University of Technology, Vienna A-1040, Austria;* orcid.org/0000-0001-5410-1067; Email: markus.valtiner@tuwien.ac.at

Authors

Gastelle F. Tiétcha − *Institute of Applied Physics, Vienna University of Technology, Vienna A-1040, Austria; Dörken MKS-Systeme GmbH & Co. KG, D-58313 Herdecke, Germany*

Dominik Dworschak − *Institute of Applied Physics, Vienna University of Technology, Vienna A-1040, Austria*

Marcel Roth − *Dörken MKS-Systeme GmbH & Co. KG, D-58313 Herdecke, Germany*

Complete contact information is available at: https://pubs.acs.org/10.1021/acsami.0c04263

Notes

The authors declare no competing financial interest.

ACKNOWLEDGMENTS

XPS measurements were performed with the support of CEITEC Nano Research Infrastructure (ID LM2015041, MEYS CR, 2016−2019), CEITEC Brno University of Technology. The authors thank the mechanical workshop at the Institute for Applied Physics for their craftsmanship. The authors acknowledge the TU Wien University Library for financial support through its Open Access Funding Program.

REFERENCES

(1) Ismail, I. M.; Abdel-Salam, O.; Ahmed, T. S.; Soliman, A.; Al-Ebrahim, M. F.; Khattab, I. A. Investigation of the Anodic Dissolution of Zinc in Sodium Chloride Electrolyte − a Green Process. *IOSR J. Appl. Chem.* **2013**, *6*, 24.

(2) Mokaddem, M.; Volovitch, P.; Ogle, K. The Anodic Dissolution of Zinc and Zinc Alloys in Alkaline Solution. I. Oxide Formation on Electrogalvanized Steel. *Electrochim. Acta* **2010**, *55* (27), 7867−7875.

(3) Vu, T. N.; Mokaddem, M.; Volovitch, P.; Ogle, K. The Anodic Dissolution of Zinc and Zinc Alloys in Alkaline Solution. Ii. Al and Zn Partial Dissolution from 5% Al−Zn Coatings. *Electrochim. Acta* **2012**, *74*, 130−138.

(4) Tuaweri, T. J.; Adigio, E. M.; Jombo, P. P. A Study of Process Parameters for Zinc Electrodeposition from a Sulphate Bath. *IJESI* **2013**, *2* (8), 17−24.

(5) Byk, T. V.; Gaevskaya, T. V.; Tsybulskaya, L. S. Effect of Electrodeposition Conditions on the Composition, Microstructure, and Corrosion Resistance of Zn−Ni Alloy Coatings. *Surf. Coat. Technol.* **2008**, *202* (24), 5817−5823.

(6) Gavrila, M.; Millet, J. P.; Mazille, H.; Marchandise, D.; Cuntz, J. M. Corrosion Behaviour of Zinc−Nickel Coatings, Electrodeposited on Steel. *Surf. Coat. Technol.* **2000**, *123* (2), 164−172.

(7) Kim, H.; Popov, B. N.; Chen, K. S. Comparison of Corrosion-Resistance and Hydrogen Permeation Properties of Zn−Ni, Zn−Ni−Cd and Cd Coatings on Low-Carbon Steel. *Corros. Sci.* **2003**, *45* (7), 1505−1521.

(8) Shen, C.; Li, X.; Li, N.; Xie, K.; Wang, J.-G.; Liu, X.; Wei, B. Graphene-Boosted, High-Performance Aqueous Zn-Ion Battery. *ACS Appl. Mater. Interfaces* **2018**, *10* (30), 25446−25453.

(9) Foroozan, T.; Yurkiv, V.; Sharifi-Asl, S.; Rojaee, R.; Mashayek, F.; Shahbazian-Yassar, R. Non-Dendritic Zn Electrodeposition Enabled by Zincophilic Graphene Substrates. *ACS Appl. Mater. Interfaces* **2019**, *11* (47), 44077−44089.

(10) Moreno-Garcia, P.; Schlegel, N.; Zanetti, A.; Cedeno Lopez, A.; Gálvez-Vázquez, M. d. J.; Dutta, A.; Rahaman, M.; Broekmann, P. Selective Electrochemical Reduction of Co2 to Co on Zn-Based Foams Produced by Cu2+ and Template-Assisted Electrodeposition. *ACS Appl. Mater. Interfaces* **2018**, *10* (37), 31355−31365.

(11) Tian, G.; Zhang, M.; Zhao, Y.; Li, J.; Wang, H.; Zhang, X.; Yan, H. High Corrosion Protection Performance of a Novel Non-fluorinated Biomimetic Superhydrophobic Zn−Fe Coating with Echinopsis Multiplex-Like Structure. *ACS Appl. Mater. Interfaces* **2019**, *11* (41), 38205−38217.

(12) Han, S.-D.; Rajput, N. N.; Qu, X.; Pan, B.; He, M.; Ferrandon, M. S.; Liao, v.; Persson, K. A.; Burrell, A. K. Origin of Electrochemical, Structural, and Transport Properties in Nonaqueous Zinc Electrolytes. *ACS Appl. Mater. Interfaces* **2016**, *8* (5), 3021−3031.

(13) Jelinek, T. W. *Galvanische Verzinkung. Elektrolyte, Nachbehandlung, Anwendung*; Eugen G. Leuze Verlag, 1st ed.; 2003; p 21.

(14) Yli-Pentti, A. 4.11 - Electroplating and Electroless Plating. In *Comprehensive Materials Processing*; Hashmi, S., Batalha, G. F., Van Tyne, C. J., Yilbas, B., Eds.; Elsevier: Oxford, 2014; pp 277−306.
(15) Fordyce, J. S.; Baum, R. L. Vibrational Spectra of Solutions of Zinc Oxide in Potassium Hydroxide. *J. Chem. Phys.* **1965**, *43* (3), 843−846.
(16) Newman, G. H.; Blomgren, G. E. Nmr Study of Complex Ions in the Aqueous Zno−Koh System. *J. Chem. Phys.* **1965**, *43* (8), 2744−2747.
(17) Dirkse, T. P. The Nature of the Zinc-Containing Ion in Strongly Alkaline Solutions. *J. Electrochem. Soc.* **1954**, *101* (6), 328−331.
(18) Maslii, A. N.; Shapnik, M. S.; Kuznetsov, M. Electroreduction of Zn(Ii) Hydroxy-Complexes in Aqueous Electrolytes: A Quantum-Chemical Study. *Russ. J. Electrochem.* **2001**, *37* (6), 615−622.
(19) Gerischer, H. Mechanism of Electrolytic Deposition and Dissolution of Metals. *Anal. Chem.* **1959**, *31* (1), 33−39.
(20) Matsuda, H.; Ayabe, Y. Polarographische Untersuchungen Über Die Kinetik Der Entladung Von Komplex-Metallionen, Insbesondere Von Hydroxo-Und Ammin-Komplexen Des Zinks. *Ber. Bunsenges. Phys. Chem.* **1959**, *63* (9−10), 1164−1171.
(21) Bockris, J. M.; Nagy, Z.; Damjanovic, A. On the Deposition and Dissolution of Zinc in Alkaline Solutions. *J. Electrochem. Soc.* **1972**, *119* (3), 285−295.
(22) Hendrikx, J.; van der Putten, A.; Visscher, W.; Barendrecht, E. The Electrodeposition and Dissolution of Zinc and Amalgamated Zinc in Alkaline Solutions. *Electrochim. Acta* **1984**, *29* (1), 81−89.
(23) Rethinam, A. J.; Ramesh Bapu, G. N. K.; Muralidharan, V. S. Role of Triethanolamine and Furfuraldehyde on the Electrochemical Deposition and Dissolution Behaviour of Zinc. *Indian J. Chem. Technol.* **2004**, *11*, 207−212.
(24) Oniciu, L.; Mureşan, L. Some Fundamental Aspects of Levelling and Brightening in Metal Electrodeposition. *J. Appl. Electrochem.* **1991**, *21* (7), 565−574.
(25) Pushpavanam, M.; Shanmugasigamani. Role of Additives in Bright Zinc Deposition from Cyanide Free Alkaline Baths. *J. Appl. Electrochem.* **2006**, *36* (3), 315−322.
(26) Rethinam, A. J.; Bapu, G. N. K. R.; Muralidharan, V.S. Role of Addition Agents in Zincate Bath- a Cyclic Voltammetry Study. *Trans. Inst. Met. Finish.* **2003**, *81* (4), 136−140.
(27) Ortiz-Aparicio, J. L.; Meas, Y.; Trejo, G.; Ortega, R.; Chapman, T. W.; Chainet, E.; Ozil, P. Effect of Aromatic Aldehydes on the Electrodeposition of Znco Alloy from Cyanide-Free Alkaline-Gluconate Electrolytes. *J. Appl. Electrochem.* **2011**, *41* (6), 669−679.
(28) Pushpavanam, M. Role of Additives in Bright Zinc Deposition from Cyanide Free Alkaline Baths. *J. Appl. Electrochem.* **2006**, *36* (3), 315−322.
(29) Ortiz-Aparicio, J. L.; Meas, Y.; Chapman, T. W.; Trejo, G.; Ortega, R.; Chainet, E. Electrodeposition of Zinc in the Presence of Quaternary Ammonium Compounds from Alkaline Chloride Bath. *J. Appl. Electrochem.* **2015**, *45*, 67−78.
(30) Diggle, J. W.; Damjanovic, A. The Inhibition of the Dendritic Electrocrystallization of Zinc from Doped Alkaline Zincate Solutions. *J. Electrochem. Soc.* **1972**, *119* (12), 1649−1658.
(31) Bressan, J.; Wiart, R. Inhibited Zinc Electrodeposition: Electrode Kinetics and Deposit Morphology. *J. Appl. Electrochem.* **1979**, *9* (1), 43−53.
(32) Chai, L.; Klein, J. Large Area, Molecularly Smooth (0.2 Nm Rms) Gold Films for Surface Forces and Other Studies. *Langmuir* **2007**, *23* (14), 7777−7783.
(33) Reviakine, I.; Johannsmann, D.; Richter, R. P. Hearing What You Cannot See and Visualizing What You Hear: Interpreting Quartz Crystal Microbalance Data from Solvated Interfaces. *Anal. Chem.* **2011**, *83* (23), 8838−8848.
(34) Seah, M. P.; Gilmore, I. S.; Beamson, G. Xps: Binding Energy Calibration of Electron Spectrometers 5?Re-Evaluation of the Reference Energies. *Surf. Interface Anal.* **1998**, *26* (9), 642−649.
(35) Zuo, J.; Erbe, A. Optical and Electronic Properties of Native Zinc Oxide Films on Polycrystalline Zn. *Phys. Chem. Chem. Phys.* **2010**, *12* (37), 11467−11476.
(36) Li, F.; Pincet, F. Confinement Free Energy of Surfaces Bearing End-Grafted Polymers in the Mushroom Regime and Local Measurement of the Polymer Density. *Langmuir* **2007**, *23* (25), 12541−12548.
(37) Jones, R. A. L. Tethered Polymer Chains in Solutions and Melts. In *Polymers at Surfaces and Interfaces*; Cambridge University Press: 1999.
(38) Bard, A. J.; Faulkner, L. R. Electroactive Layers and Modified Electodes. In *Electrochemical Methods: Fundamentals and Applications*, 2nd ed.; Wiley Textbooks: 2000.
(39) Hamann, C. H.; Hamnett, A.; Vielstich, W. Electrical Potentials and Electrical Current. In *Electrochemistry*, 2nd ed.; Wiley: 2007.
(40) Israelachvili, J. N. *Intermolecular and Surface Forces*, 3rd ed.; Academic Press: 2011.
(41) Housecroft, C. E.; Constable, E. C. Coordination Complexes of the D-Block Metals. In *An Introduction to Organic, Inorganic and Physical Chemistry*, 3rd ed.; Prentice Hall: 2005.
(42) Gade, L. H. *Koordinationschemie*; Wiley-VCH Verlag GmbH: 2013.
(43) Rodriguez, J. A.; Hrbek, J. Metal−Metal Bonding on Surfaces: Zn−Au on Ru(001). *J. Chem. Phys.* **1992**, *97* (12), 9427−9439.
(44) Carvalhal, R. F.; Sanches Freire, R.; Kubota, L. T. Polycrystalline Gold Electrodes: A Comparative Study of Pretreatment Procedures Used for Cleaning and Thiol Self-Assembly Monolayer Formation. *Electroanalysis* **2005**, *17*, 1251−1259.
(45) Doi, M.; Edwards, S. F. The Zimm Model. In *The Theory of Polymer Dynamics*; Clarendon Press: 1988.

https://dx.doi.org/10.1021/acsami.0c04263
ACS Appl. Mater. Interfaces 2020, 12, 29928−29936